Inorg. Chem. **2006**, *45*, 9006–9013

Development of Organometallic Ruthenium–Arene Anticancer Drugs That Resist Hydrolysis

Wee Han Ang,[†] Elisa Daldini,[†] Claudine Scolaro,[†] Rosario Scopelliti,[†] Lucienne Juillerat-Jeannerat,[‡] and Paul J. Dyson*,[†]

Institut des Sciences et Ingénierie Chimiques, Ecole Polytechnique Fédérale de Lausanne (EPFL), CH-1015 Lausanne, Switzerland, and University Institute of Pathology, Centre Hospitalier Universitaire Vaudois (CHUV), CH-1011 Lausanne, Switzerland

Received June 7, 2006

With a view to develop drugs that could resist hydrolysis in aqueous media, organometallic arene-capped ruthenium(II) 1,3,5-triaza-7-phosphatricyclo[3.3.1.1]decane (RAPTA) complexes bearing chelating carboxylate ligands have been prepared and studied. The new complexes, Ru(η^6-cymene)(PTA)(C_2O_4) (**1**) and Ru(η^6-cymene)(PTA)($C_6H_6O_4$) (**2**), were found to be highly soluble and kinetically more stable than their RAPTA precursor that contains two chloride ligands in place of the carboxylate ligands. They were also able to resist hydrolysis in water and exhibited significantly lower pK_a values. Importantly, they showed a similar order of activity in inhibiting cancer cell-growth proliferation (as determined by in vitro assays) and exhibited oligonucleotide binding characteristics (as evidenced by matrix-assisted laser desorption ionization mass spectrometry) similar to those of the RAPTA precursor, hence realizing a strategy for developing a new generation of stable and highly water-soluble RAPTA adducts.

Introduction

Since the discovery that *cisplatin* could inhibit tumor growth some 40 years ago, it has become one of the most widely used anticancer drugs, often as part of the first line of treatment against various tumors.[1−3] However, there are inherent limitations with cisplatin, primarily its high toxicity, leading to unwanted side effects, and low administration dosage.[1,4] This has led to the development of drugs based on other transition metals.[3,5,6] In particular, cytotoxic drugs based on ruthenium have shown the greatest potential and remain the subject of extensive drug discovery efforts.[5,7,8] There are presently two such drugs, namely, NAMI-A and KP1019, undergoing clinical evaluation against metastatic tumors and colon cancers, respectively.[9] The compounds are characterized by their low general toxicity, which has been attributed to the ability of ruthenium to accumulate specifically in cancer tissues, possibly via the transferrin pathway.[3,5,10,11]

Another series of ruthenium compounds that have been extensively studied for anticancer activity is the RAPTA (ruthenium−arene 1,3,5-triaza-7-phosphatricyclo[3.3.1.1]-decane) series of compounds, based on an arene-capped ruthenium(II) center (see Chart 1).[12−16] These compounds show high selectivity toward cancer cell lines in vitro, and

* To whom correspondence should be addressed. E-mail: paul.dyson@epfl.ch. Phone: +41 (0) 21 693 9854. Fax: +41 (0) 21 693 9885.
[†] EPFL.
[‡] CHUV.

(1) Boulikas, T.; Vougiouka, M. *Oncol. Rep.* **2003**, *10*, 1663−1682.
(2) Wong, E.; Giandomenico, C. M. *Chem. Rev.* **1999**, *99*, 2451−2466.
(3) Galanski, M.; Arion, V. B.; Jakupec, M. A.; Keppler, B. K. *Curr. Pharm. Des.* **2003**, *9*, 2078−2089.
(4) (a) Fuertes, M. A.; Alonso, C.; Perez, J. M. *Chem. Rev.* **2003**, *103*, 645−662. (b) Agarwal, R.; Kaye, S. B. *Nat. Rev. Cancer* **2003**, *3*, 502−516.
(5) Clarke, M. J.; Zhu, F. C.; Frasca, D. R. *Chem. Rev.* **1999**, *99*, 2511−2533.
(6) Fish, R. H.; Jaouen, G. *Organometallics* **2003**, *22*, 2166−2177.
(7) Melchart, M.; Sadler, P. J. In *Bioorganometallics: Biomolecules, Labeling, Medicine*; Jaouen, G., Ed.; Wiley-VCH: New York, 2006; pp 39−62.
(8) Yan, Y. K.; Melchart, M.; Habtemariam, A.; Sadler, P. J. *Chem. Commun.* **2005**, 4764−4776.
(9) (a) Bergamo, A.; Gava, B.; Alessio, E.; Mestroni, G.; Serli, B.; Cocchietto, M.; Zorzet, S.; Sava, G. *Int. J. Oncol.* **2002**, *21*, 1331−1338. (b) Kapitza, S.; Pongratz, M.; Jakupec, M. A.; Heffeter, P.; Berger, W.; Lackinger, L.; Keppler, B. K.; Marian, B. *J. Cancer Res. Clin. Oncol.* **2005**, *131*, 101−110.
(10) Dyson, P. J.; Sava, G. *Dalton Trans.* **2006**, 1929−1933.
(11) (a) Allardyce, C. S.; Dorcier, A.; Scolaro, C.; Dyson, P. J. *Appl. Organomet. Chem.* **2005**, *19*, 1−10. (b) Khalaila, I.; Allardyce, C. S.; Verma, C. S.; Dyson, P. J. *ChemBioChem* **2005**, *6*, 1788−1795.
(12) Serli, B.; Zangrando, E.; Gianferrara, T.; Scolaro, C.; Dyson, P. J.; Bergamo, A.; Alessio, E. *Eur. J. Inorg. Chem.* **2005**, 3423−3434.
(13) (a) Scolaro, C.; Geldbach, T. J.; Rochat, S.; Dorcier, A.; Gossens, C.; Bergamo, A.; Cocchietto, M.; Tavernelli, I.; Sava, G.; Rothlisberger, U.; Dyson, P. J. *Organometallics* **2006**, *25*, 756−765. (b) Dorcier, A.; Dyson, P. J.; Gossens, C.; Rothlisberger, U.; Scopelliti, R.; Tavernelli, I. *Organometallics* **2005**, *24*, 2114−2123.

10.1021/ic061008y CCC: $33.50
Published on Web 09/29/2006

Chart 1

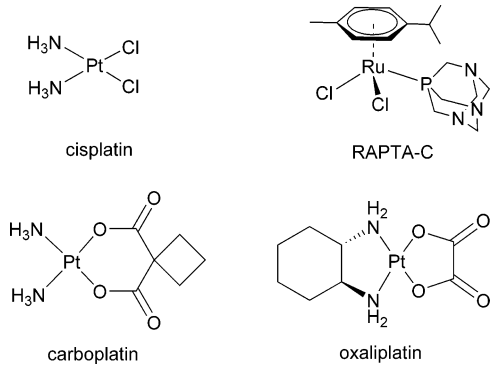

in vivo they effectively reduce lung metastases in mice without significantly affecting the primary tumor.[14] In keeping with the two ruthenium drugs under clinical trials, the RAPTA compounds are well tolerated in vivo. However, the RAPTA complexes are prone to hydrolysis and would have to be administered in saline to suppress the cleavage of the chloride ligands. The presence of hydrolysis products, which are often difficult to characterize, would be problematic for pharmacokinetics studies and could jeopardize clinical evaluation trials.

It is therefore desirable to develop RAPTA complexes that could resist hydrolysis. One strategy is to replace the labile chloride ligands with bidentate ligands and exploit the favorable thermodynamics of a chelating arrangement to stabilize the ruthenium coordination sites. However, the choice of ligands is important because a ligand bound too strongly could render the drug inactive, while a labile ligand could be easily hydrolyzed or replaced. Bidentate carboxylate ligands have been used to endow cisplatin derivatives with high aquatic solubility and resistance to hydrolysis.[17] Two such examples, *carboplatin* and *oxaliplatin* (see Chart 1), are being used routinely in clinical practice. Carboplatin, in particular, is found to be much less toxic than cisplatin and may be administered at higher doses, although it is active in the same range of tumors as cisplatin.[2] We report the use of bidentate carboxylate ligands to develop novel RAPTA complexes with properties similar to those of related platinum species and herein describe the outcome of this study.

Results and Discussion

Reaction of the dimer, $[(\eta^6\text{-cymene})RuCl(\mu\text{-}Cl)]_2$, with an excess of silver oxalate or 1,1-cyclobutanedicarboxylate in a polar solvent, followed by treatment with stiochiometric amounts of 1,3,5-triaza-7-phosphatricyclo[3.3.1.1]decane (PTA), affords the complexes $Ru(\eta^6\text{-cymene})(PTA)(C_2O_4)$ (**1**) and $Ru(\eta^6\text{-cymene})(PTA)(C_6H_6O_4)$ (**2**) in good yield. In contrast to the triphenylphosphine analogues, the complexes could not be prepared directly from the reaction of $Ru(\eta^6\text{-cymene})(PTA)Cl_2$ (RAPTA-C) with the silver carboxylates, presumably because the coordinated PTA interacts with the Ag^I ions.[18] The choice of solvent was also important for the formation of monomeric species in order to avoid the formation of bridging $[(\eta^6\text{-cymene})Ru]$ moieties (Scheme 1).

Scheme 1. Synthesis of **1** and **2**

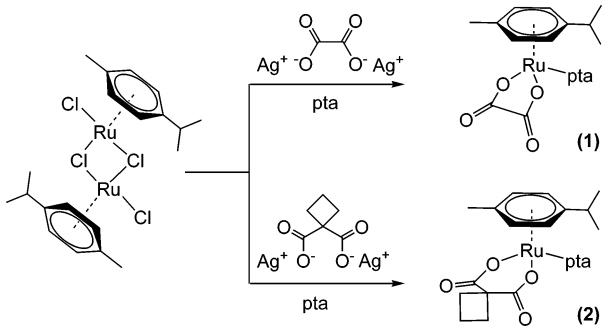

The compounds were characterized by ^1H, ^{31}P, and ^{13}C NMR spectroscopy and electrospray ionization mass spectrometry (ESI-MS). In deuterated chloroform, both complexes exhibited a singlet in their ^{31}P NMR spectra (−34.05 ppm for **1** and −30.16 ppm for **2**) that is shifted to lower frequency compared to RAPTA-C (−36.24 ppm).[15] This is anticipated given the deshielding effect of the electron-withdrawing carboxylate groups. ^{13}C NMR spectroscopy also indicated the presence of the carboxylate ligands with characteristic peaks between 160 and 180 ppm. In the ^1H NMR of **2**, two triplets were observed at 2.76 and 2.66 ppm, which are attributed to the two $-CH_2-$ groups on the 1 and 3 positions of the cyclobutane ring. In an aqueous solution of sodium 1,1-cyclobutanedicarboxylate, these groups are equivalent, but upon coordination, they become stereotropic. Complexes **1** and **2** were also found to be extremely soluble in water, at more than 100 mM concentration levels, some 5−10 times more soluble than RAPTA-C.

Single crystals of **1** were grown by vapor diffusion of diethyl ether into a saturated solution of **1** in dichloromethane. The structure of **1** is illustrated in Figure 1, and key bond lengths and angles are given in the caption. The bond lengths are essentially of typical values, although the O1−Ru1−O2 bond angle of 78.43(7)° is significantly smaller than 90°, indicating that the five-membered metallacycle is strained. In comparison, the chloride ligands on RAPTA-C are displaced at a less strained bond angle of 89.16(4)°.

To study the dissolution characteristics of **1** and **2** in aqueous media, the complexes were dissolved in water and monitored by ^{31}P NMR spectroscopy and ESI-MS. Complex **1** exhibits a singlet at −33.93 ppm, indicating that only one species is present, i.e., the parent compound without having undergone hydrolysis. The ESI-MS spectrum contains mass peaks consistent with solvated and aggregated species of **1** with Na^+, H^+, and $HNEt_3^+$ ions, which were further verified

(14) Scolaro, C.; Bergamo, A.; Brescacin, L.; Delfino, R.; Cocchietto, M.; Laurenczy, G.; Geldbach, T. J.; Sava, G.; Dyson, P. J. *J. Med. Chem.* **2005**, *48*, 4161−4171.
(15) Allardyce, C. S.; Dyson, P. J.; Ellis, D. J.; Salter, P. A.; Scopelliti, R. *J. Organomet. Chem.* **2003**, *668*, 35−42.
(16) Allardyce, C. S.; Dyson, P. J.; Ellis, D. J.; Heath, S. L. *Chem. Commun.* **2001**, 1396−1397.
(17) (a) Pasini, A.; Zunino, F. *Angew. Chem., Int. Ed. Engl.* **1987**, *26*, 615−624. (b) Harrison, R. C.; Mcauliffe, C. A. *Inorg. Chim. Acta* **1980**, *46*, L15−L16.
(18) Davies, D. L.; Fawcett, J.; Krafczyk, R.; Russell, D. R.; Singh, K. *J. Chem. Soc., Dalton Trans.* **1998**, 2349−2352.

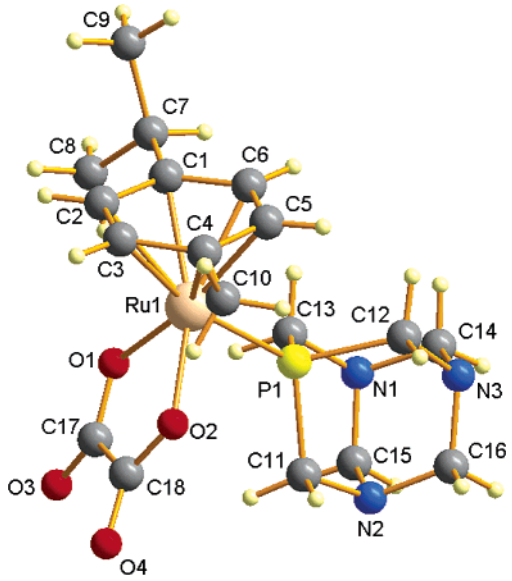

Figure 1. (a) Ball-and-stick representation of **1**; atoms as spheres of arbitrary diameter. Key bond lengths (Å) and angles (deg): Ru1−cymene$_{centroid}$, 1.69; Ru1−P1, 2.310(1); Ru1−O1, 2.093(2); Ru1−O1, 2.095-(1); C17−O1, 1.288(4); C17−O3, 1.232(3); C18−O2, 1.288(3); C18−O3, 1.227(3); O1−Ru1−O2, 78.43(7); P1−Ru1−O1, 82.83(5); P1−Ru1−O1, 88.79(5).

by fragmentation analyses. Complex **2**, however, exhibited two peaks in the ^{31}P NMR spectrum with a minor peak (2%) at −28.87 ppm, at slightly lower frequency to the main peak at −29.73 ppm, indicating possible hydrolysis products. In the ESI-MS spectrum, besides the anticipated parent mass peaks, a peak at *m*/*z* 523 was also observed and is attributable to the dimer $[\{(\eta^6\text{-cymene})\text{Ru}\}_2(\text{OH})_3]^+$. However, the formation of the hydroxo-bridged dimer appears to be an artifact of the mass spectrometry, which injects the sample at 100 °C. In fact, the ESI-MS spectrum of RAPTA-C under the same conditions shows the peaks corresponding to the hydroxy-bridged dimer with a relative intensity of c.a. 50%, and that of $[(\eta^6\text{-cymene})\text{RuCl}(\mu\text{-Cl})]_2$ in water is comprised almost exclusively of the hydroxo-bridged species. It is, however, noteworthy that the peaks corresponding to this species were not observed in the ESI-MS spectrum of **1**.

To study the kinetic stability of new complexes relative to RAPTA-C, ligand exchange between the two chloride ligands on RAPTA-C and sodium oxalate or 1,1-cyclobutanedicarboxylate was studied using UV−vis and ^{31}P NMR spectroscopy. The aqueous medium contained 100 mM NaCl in order to suppress the immediate hydrolysis of RAPTA-C in water. RAPTA-C was reacted with 100-fold excess of the respective sodium carboxylate at 25 °C, and UV−vis absorption spectra were recorded at regular time intervals (see Figure 2, top). The absorption maxima for complexes **1** and **2** in a 100 mM NaCl solution were determined to be 302.5 and 317.5 nm, respectively. The absorbances at these absorption maxima were extracted from the time course UV−vis datasets and plotted against time, as shown in Figure 2. The curves obtained could be fitted using pseudo-first-

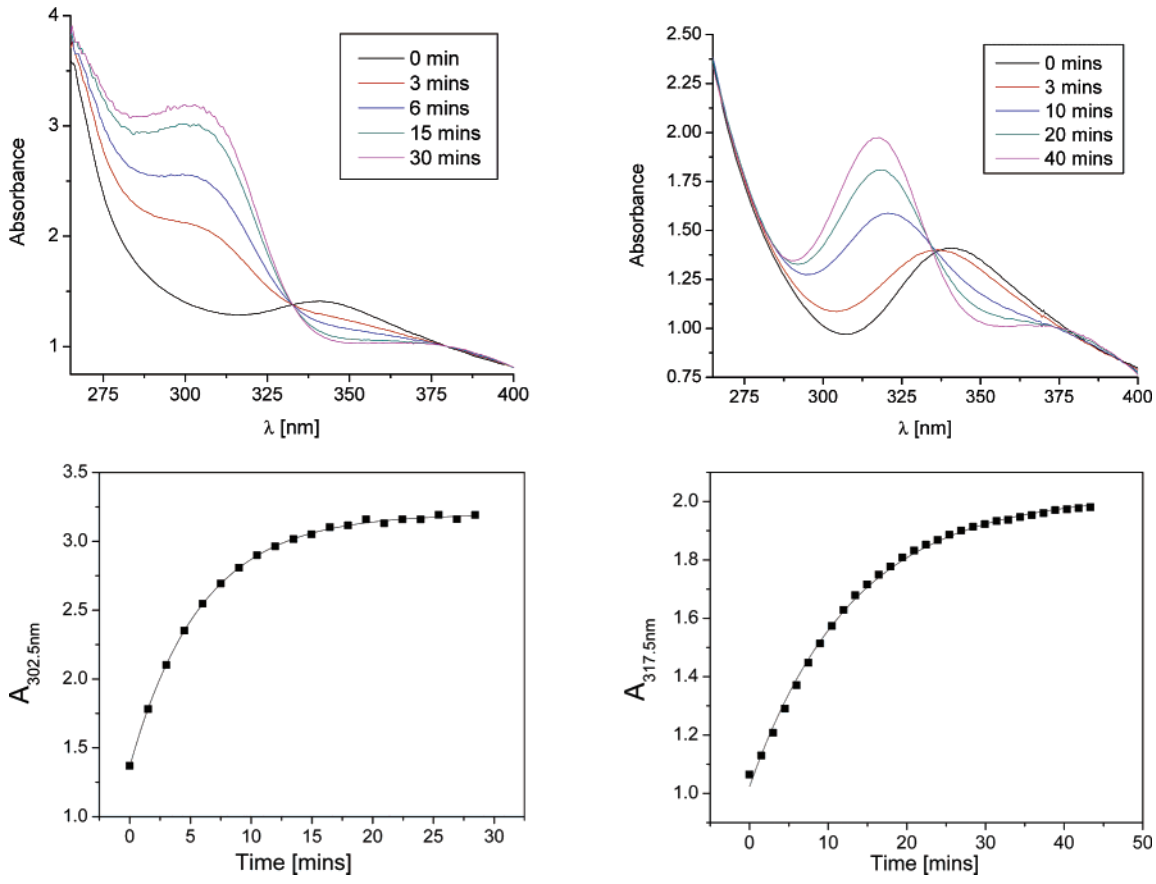

Figure 2. Time-course UV absorption spectra from the reaction of RAPTA-C with sodium oxalate (top, left) and sodium 1,1-cyclobutadicarboxylate (top, right) between 260 and 400 nm at 25 °C. Plot of absorption maxima of the reaction of RAPTA-C with sodium oxalate (bottom, left) and sodium 1,1-cyclobutadicarboxylate (bottom, right) vs time.

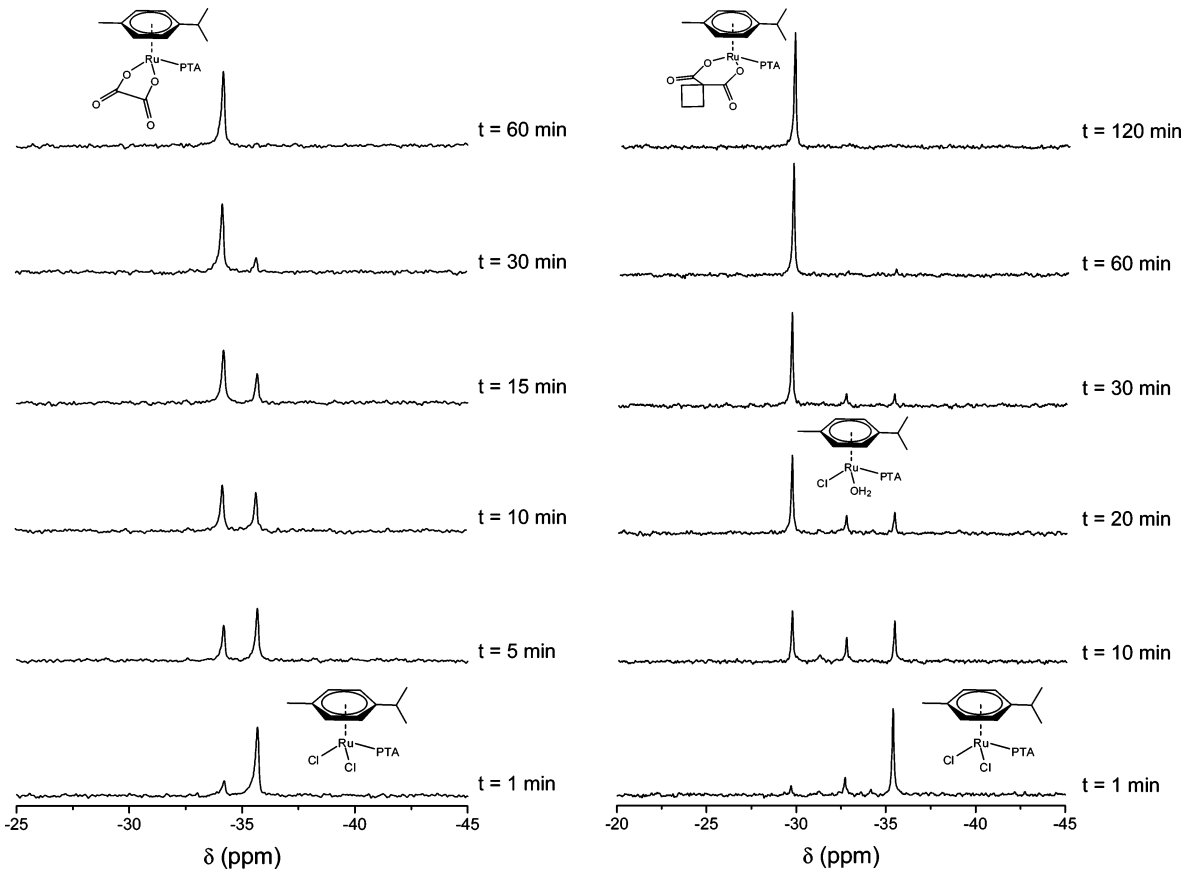

Figure 3. $^{31}P\{^{1}H\}$ NMR spectra from the reaction of RAPTA-C with sodium oxalate (left) and sodium 1,1-cyclobutadicarboxylate (right). Spectra were acquired for 1.45 min at 5-min intervals. The denoted time is at the commencement of the spectral acquisition.

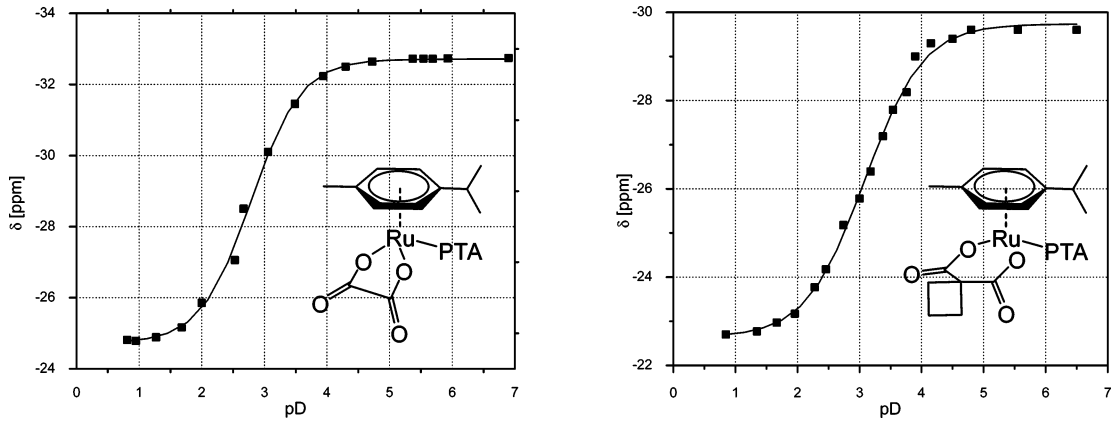

Figure 4. Plot of $\delta[^{31}P]$ vs p*D* of **1** (left) and **2** (right).

order reaction kinetics. The half-life, $t_{1/2}$, of RAPTA-C (1 mM) in solution in the presence of 100-fold excess of sodium oxalate was found to be 4.0 min, and $t_{1/2}$ for RAPTA-C in 100-fold excess of sodium 1,1-cyclobutanedicarboxylate is 9.0 min at 25 °C. The preference for complexes **1** and **2**, at equimolar concentrations of sodium chloride and sodium carboxylate, suggests that the new complexes are significantly more kinetically stable than RAPTA-C. The more rapid formation of complex **1** also suggests that it is more stable than **2**.

The ligand-exchange reactions were also followed using ^{31}P NMR in order to identify any intermediate species involved. The experiments were conducted at a higher concentration of RAPTA-C, i.e., 10 mM, to improve the sensitivity of the ^{31}P NMR signal (Figure 3). While RAPTA-C was converted directly to **1**, an intermediate species was detected at −33.30 ppm in the reaction of RAPTA-C with sodium 1,1-cyclobutanedicarboxylate, which is consistent with the chemical shift of monohydrated RAPTA-C [(η^6-cymene)Ru(PTA)(OH_2)Cl]$^+$. A possible explanation for the occurrence of the hydrated species could be due to the hydrolysis of the monochelated [(η^6-cymene)Ru(PTA)(η^1-$C_6H_4O_4$)Cl]$^-$ intermediate. For **1**, the rigid oxalate structure would encumber the free carboxylic group within the proximity of the ruthenium coordination sphere once the first carboxylic group is coordinated, thus favoring rapid substitution of the second chloride. In contrast for **2**, the more flexible and open 1,1-cyclobutanedicarboxylate ligand could

Table 1. pK_a Values for Complexes **1** and **2** in a 0.1 M NaCl Solution

complex	pK_a
PTA	5.63 ± 0.05
RAPTA-C	3.13 ± 0.02
1	2.35 ± 0.02
2	2.64 ± 0.03

result in a less favorable arrangement with respect to the second chloride substitution and at a time scale sufficient to observe the hydrolysis intermediate. However, it is evident that the chelate arrangement is still strongly favored and the reaction reaches completion after 2 h with the exclusive formation of compound **2**.

The pK_a values of the coordinated PTA ligands in **1** and **2** were determined using ^{31}P NMR spectroscopy in D_2O by measuring the chemical shift of the complexes at different p*D* values. The values obtained were plotted as chemical shift vs p*D* (see Figure 4) and fitted using the Henderson−Hasselbach equation. The pK_a value is obtained at the midpoint of the curve, with 0.44 being subtracted to account for the difference between the pH and p*D*.[14] The pK_a values of the free and coordinated ligands are summarized in Table 1. The values for complexes **1** and **2** are significantly lower than those of RAPTA-C, suggesting that the new complexes are stable at lower pH values before being protonated. Furthermore, their stability at low pH indicates that oral administration, which involves transit through the low-pH environment of the stomach, should be possible.

It is generally believed that the target of organometallic ruthenium drugs within the cell, including RAPTA-C, is DNA or RNA. Indeed, previous studies have demonstrated the facile complexation of RAPTA-C and its derivatives with single-strand DNA (ssDNA) models, although an unequivocal preferential binding site could not be ascertained.[13] To study the impact of ligand substitution on the reactivity of RAPTA-C toward ssDNA, the 14-mer 5′-ATACATGGTACATA oligonucleotide was incubated with a 5-fold molar concentration of RAPTA-C, **1**, or **2** for 24 h and analyzed directly using matrix-assisted laser desorption ionization time-of-flight (MALDI-TOF) MS. Multiple adducts of the drugs with the 14-mer were observed and could be assigned (see Table 2). It was evident that the majority of adducts formed upon complexation with RAPTA-C involved the loss of the chloride ligands and, to a smaller extent, the loss of either the arene ring and/or the PTA ligand. A similar trend was also observed when the oligonucleotide was incubated with **1** and **2**, i.e., loss of the carboxylate ligand and, to a lesser extent, loss of the arene and/or the PTA moieties. These data indicate that the substitution of the chloride ligands on RAPTA-C by the bidentate carboxylate ligands had minimal impact on their mode of reactivity with ssDNA, suggesting that in the presence of an appropriate donor the carboxylate may be displaced, possibly via a hydrolysis intermediate or perhaps a mechanism involving arene slippage to create a vacant coordination site.

The impact of the ligand modification on the anticancer activity of the complexes relative to RAPTA-C (proven in vivo) was undertaken by testing for inhibition of cell proliferation activity against the HT29 colon carcinoma, the A549 lung carcinoma, and the T47D and MCF7 breast carcinoma cell lines (see Figure 5 and Table 3). The compounds were found to retain an order of activity remarkably similar to that of RAPTA-C. This similar activity, in terms of reactivity with ssDNA and in vitro inhibition of cell proliferation, indicates that the ligand modification is not detrimental to the function of the complexes as anticancer drugs. It is worth noting that such high IC_{50} values are typical of RAPTA compounds and also the clinically proven ruthenium complex NAMI-A. Despite such high IC_{50} values, they have excellent activity in vivo against secondary (metastatic) tumor cells.[10]

Conclusions

Second-generation organometallic ruthenium-based anticancer drugs based on the RAPTA system have been synthesized, characterized, and tested against four cancer cell lines. The new complexes maintain essentially the same order of cell-growth inhibition activity against cancer cells as RAPTA-C and were found to share similar modes of reactivity with oligonucleotides. More importantly, they were found to resist hydrolysis, and they are stable at low pH,

Table 2. Oligonucleotides Observed by MALDI-TOF MS after Incubation of the 14-mer 5′-ATACATGGTACATA with RAPTA-C, **1**, or **2** (1:5 Oligonucleotide Drug Ratio)

complex	calcd *m*/*z*	obsd *m*/*z*	relative abundance (%)[a]	oligonucleotide species assignment
RAPTA-C	4269.8	4268.3		[14-mer]
	4505.1	4504.9	31	[14-mer + Ru(η^6-*p*-cymene)]
	4528.0	4525.5	23	[14-mer + Ru(PTA)]
	4662.2	4660.6	42	[14-mer + Ru(η^6-*p*-cymene)(PTA)]
	4697.7	4696.2	19	[14-mer + Ru(η^6-*p*-cymene)(PTA) + Cl]
1	4269.8	4269.8		[14-mer]
	4505.1	4505.4	16	[14-mer + Ru(η^6-*p*-cymene)]
	4528.0	4527.8	12	[14-mer + Ru(PTA)]
	4662.2	4662.2	29	[14-mer + Ru(η^6-*p*-cymene)(PTA)]
	4697.7	4698.1	26	[14-mer + Ru(η^6-*p*-cymene)(PTA) + Cl]
2	4269.8	4268.0		[14-mer]
	4505.1	4502.0	37	[14-mer + Ru(η^6-*p*-cymene)]
	4528.0	4527.0	37	[14-mer + Ru(PTA)]
	4662.2	4660.7	58	[14-mer + Ru(η^6-*p*-cymene)(PTA)]
	4697.7	4696.8	26	[14-mer + Ru(η^6-*p*-cymene)(PTA) + Cl]

[a] The intensities of the oligonucleotide species relative to the parent orglionucleotide at ca. *m*/*z* 4269.

Table 3. Inhibition of Cell-Growth Proliferation Determined by the MTT Assay

	IC_{50} (μM)[a]			
complex	HT29	A549	T47D	MCF7
RAPTA-C	436	1029	1063	>1600
1	267	1130	1174	>1600
2	265	1567	1088	>1600

[a] The cells were exposed to the drugs for 72 h continuously.

which realizes a strategy for developing a new generation of RAPTA complexes. Like other types of ruthenium−arene complexes under evaluation for their anticancer activity and ruthenium complexes more generally,[3,8,19] cytotoxicities of **1** and **2** are low compared to those of platinum drugs. Nevertheless, general toxicities are also low, but the prospect of clinical applications remains high.[10]

Experimental Section

All reagents were purchased from Acros Chemicals unless otherwise indicated. $RuCl_3 \cdot xH_2O$ was obtained from Precious Metals Online. 1,1-Cyclobutanedicarboxylic acid was purchased from ABCR, and sodium oxalate was purchased from Fluka. The reactions were performed with solvents dried using appropriate reagents and distilled prior to use. RAPTA-C, PTA, and [(η^6-cymene)RuCl(μ-Cl)]$_2$ were prepared and purified according to literature procedures.[16,20] IR spectra were recorded on a Perkin-Elmer FT-IR 2000 system. NMR spectra were measured on a Bruker DMX 400 spectrometer, using $SiMe_4$ for ^{1}H and ^{13}C NMR and H_3PO_4 for ^{31}P NMR as external standards at 20 °C. Positive-mode ESI-MS spectra for synthesized compounds were recorded on a ThermoFinnigan LCQ Deca XP Plus quadrupole ion-trap instrument on samples dissolved in water with the ionization energy set at 5.0 V and the capillary temperature at 150 °C as previously described.[21] Elemental analyses were carried out at the Institute of Chemical Sciences and Engineering (EPFL).

Preparation of Sodium 1,1-Cyclobutanedicarboxylate. 1,1-Cyclobutanedicarboxylic acid (1.0 g, 6.9 mmol) was dissolved in methanol (20 mL), and 1 M methanolic NaOH (15 mL) was added. The precipitate formed was filtered and washed consecutively with methanol (50 mL) and diethyl ether (50 mL). The precipitate was dried in vacuo and used without further purification (yield: 1.04 g, 80%).

Preparation of Silver Oxalate. An aqueous solution of silver nitrate (1.86 g, 11 mmol) was added dropwise to an aqueous solution of sodium oxalate (0.67 g, 5 mmol), resulting in the immediate formation of a white precipitate. The reaction was stirred for 10 min and filtered. The white precipitate was washed with water (50 mL), dried in vacuo, and used without further purification (yield: 1.36 g, 90%).

Preparation of Silver 1,1-Cyclobutanedicarboxylate. An aqueous solution of silver nitrate (1.86 g, 11 mmol) was added dropwise to an aqueous solution of sodium 1,1-cyclobutanedicarboxylate (0.94 g, 5 mmol), resulting in the immediate formation of a white precipitate. The reaction was stirred for 10 min and then filtered. The white precipitate was washed with water (50 mL), dried in vacuo, and used without further purification (yield: 1.43 g, 80%).

(19) (a) Alessio, E.; Mestroni, G.; Bergamo, A.; Sava, G. *Curr. Top. Med. Chem.* **2004**, *4*, 1525−1535. (b) Sava, G.; Bergamo, A. *Int. J. Oncol.* **2000**, *17*, 353−365.
(20) (a) Bennett, M. A.; Smith, A. K. *J. Chem. Soc., Dalton Trans.* **1974**, 233−241. (b) Daigle, D. J. *Inorg. Synth.* **1998**, *32*, 40−45.
(21) Dyson, P. J.; McIndoe, J. S. *Inorg. Chim. Acta* **2003**, *354*, 68−74.

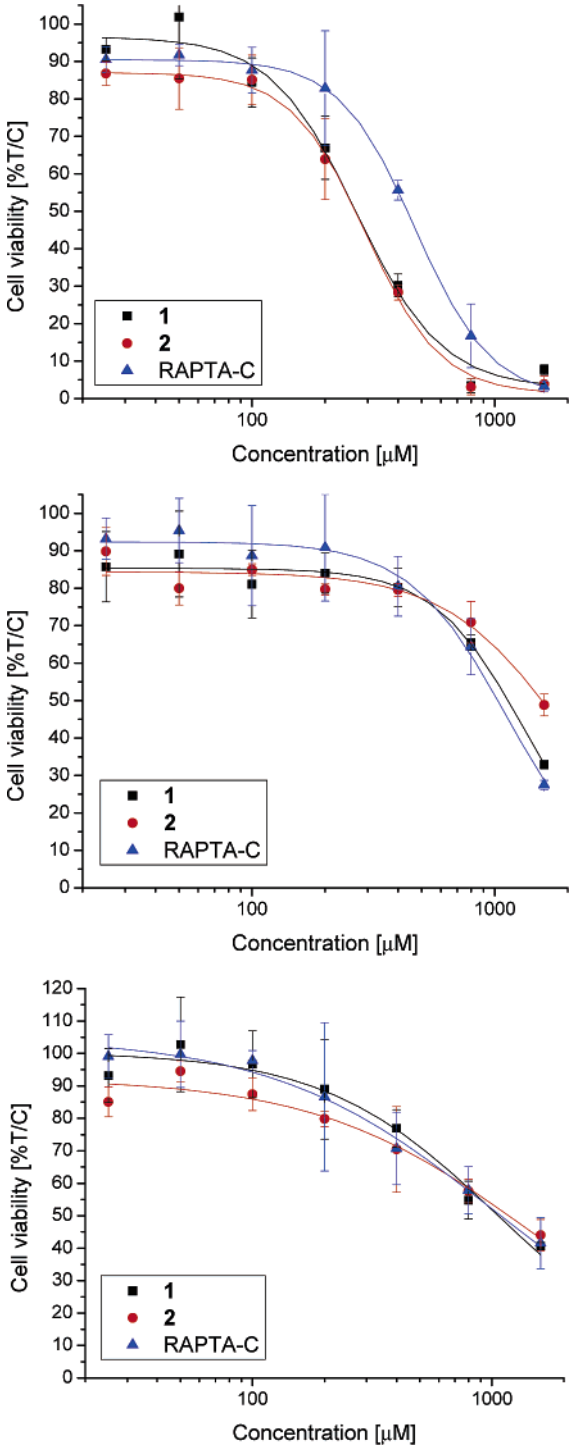

Figure 5. Dose−response curves for **1**, **2**, and RAPTA-C vs the HT29 colon carcinoma (top), A549 lung carcinoma (middle), and T47D breast carcinoma (bottom) cell lines over an exposure of 72 h.

Synthesis of OxaloRAPTA-C (1). [(η^6-Cymene)RuCl(μ-Cl)]$_2$ (196.8 mg, 0.322 mmol) and silver oxalate (240 mg, 0.797 mmol) were stirred in water for 12 h. The mixture was filtered through Celite to remove the AgCl precipitate. The solvent was removed under vacuum, and the residue was redissolved in methanol (25 mL). PTA (120 mg, 0.764 mmol) was added, and the reaction was stirred for 2 h. The solvent was reduced to ca. 5% of its original volume, and diethyl ether (25 mL) was added. The slurry was cooled to 4 °C for 12 h to complete the precipitation of the product. The precipitate was filtered and recrystallized from methanol−diethyl

ether to yield a light-orange precipitate (yield: 285 mg, 89%). Vapor diffusion of diethyl ether into a solution of **7** in dichloromethane yielded orange crystals suitable for X-ray single-crystal diffraction. ^{1}H NMR (D_2O, 400.13 MHz): δ 5.98, 5.89 (dd, 4H, Ar−*H*), 4.57 (s, 6H, PTA−N−C*H*$_2$−N), 4.15 (s, 6H, PTA−P−C*H*$_2$−N), 2.61 (septet, 1H, −C*H*(CH_3)$_2$), 2.05 (s, 3H, −*CH*$_3$), 1.22 (d, −CH(C*H*$_3$)$_2$). ^{13}C{^{1}H} NMR (D_2O, 100.63 MHz): δ 166.2 (−*C*O_2), 105.0, 97.7, 87.3, 86.8 (Ar−*C*), 70.7 (N−*C*H_2−N), 48.7 (P−*C*H_2−N), 30.8 (−Ar*CH*$_3$), 21.5 (−CH(*C*H_3)$_2$), 17.3 (-*C*H(CH_3)$_2$). ^{31}P-{^{1}H} NMR (D_2O, 400.13 MHz): δ −33.39. ESI-MS (H_2O, +ve mode): *m*/*z* 504 $[M + Na]^+$, 583 $[M + HNEt_3]^+$, 984 $[M_2 + Na]^+$. Anal. Calcd for $C_{18}H_{26}N_3O_4PRu\cdot 0.5H_2O$: C, 44.17; H, 5.56; N, 8.58. Found: C, 44.24; H, 5.58; N, 8.69.

Synthesis of CarboRAPTA-C (2). [(η^6-Cymene)RuCl(μ-Cl)]$_2$ (228 mg, 0.373 mmol) and silver 1,1-cyclobutanedicarboxylate (300 mg, 0.838 mmol) were stirred in acetonitrile (50 mL) for 12 h, during which time a yellow precipitate was formed. The solvent was removed, and the residue was redissolved in methanol (25 mL). The mixture was filtered through Celite to remove the AgCl precipitate. PTA (130 mg, 0.828 mmol) was added to the filtrate, and the solution was stirred for 2 h. The solvent was reduced to ca. 5% of its original volume, and diethyl ether (25 mL) was added. The slurry was cooled to 4 °C for 4 h to complete the precipitation of the product. The precipitate was filtered and recrystallized from dichloromethane−diethyl ether to yield an orange precipitate (yield: 288 mg, 72.2%). ^{1}H NMR ($CDCl_3$, 400.13 MHz): δ 5.54, 5.43 (dd, 4H, Ar−*H*), 4.49 (s, 6H, PTA−N−C*H*$_2$−N), 4.15 (s, 6H, PTA−P−C*H*$_2$−N), 2.76, 2.66 (t, 4H, −CH_2(C*H*$_2$)$_2$), 2.58 (septet, 1H, −C*H*(CH_3)$_2$), 2.02 (s, 3H, −*CH*$_3$), 1.94 (quintet, 2H, −C*H*$_2$-(CH_2)$_2$), 1.24 (d, −CH(C*H*$_3$)$_2$). ^{13}C{^{1}H} NMR ($CDCl_3$, 100.63 MHz): δ 178.7 (−(*C*O_2)$_2$), 102.5, 96.1, 87.9, 85.3 (Ar−*C*), 72.9 (N−*C*H_2−N), 50.8 (P−*C*H_2−N), 55.9, 35.1, 27.1, 15.2 (*C*$_4H_6$-(CO_2−)$_2$), 30.9 (−Ar*CH*$_3$), 22.3 (−CH(*C*H_3)$_2$), 17.6 (−*C*H(CH_3)$_2$). ^{31}P{^{1}H} NMR ($CDCl_3$, 400.13 MHz): δ −30.16. ESI-MS (H_2O, +ve mode): *m*/*z* 558 $[M + Na]^+$, 821 $[M_3 + (H_3O)_2]^+$, 1090 $[M_2 + H_3O]^+$, 536 $[M]^+$. Anal. Calcd for $C_{22}H_{32}N_3O_4PRu\cdot H_2O$: C, 47.73; H, 6.19; N, 7.59. Found: C, 47.99; H, 6.45; N, 7.72.

(a) Structural Characterization of 1 in the Solid State. Relevant details about the structural refinements are compiled in Table 4, and selected bond distances and angles are given in the caption of Figure 1. Data collection was performed on a four-circle Kappa goniometer equipped with an Oxford Diffraction KM4 Sapphire CCD at 140(2) K, and data reduction was performed using *CrysAlis RED*.[22] Structure solution was performed using *SiR97*,[23] and the structure was refined by full-matrix least-squares refinement (against F^2) using *SHELXTL* software.[22] All non-hydrogen atoms were refined anisotropically, while hydrogen atoms were placed in their geometrically generated positions and refined using the riding model. Empirical absorption corrections (DELABS) were applied,[24] and graphical representations of the structure were made with *Diamond*.[25]

(b) Oligonucleotide Binding. The 14-mer oligonucleotide 5′-ATACATGGTACATA-3′ was obtained from MWG Biotech AG (Ebersberg, Germany), and the concentration was taken to be 57 μM, as specified by the supplier. The samples were prepared by mixing the equivolume of 14-mer with an aqueous solution of the complex (285 μM) to achieve a stoichiometric ratio of 1:5. The MS spectra was recorded in linear mode (negative) on a Axima CFR Plus (Kratos/Shimadzu) MALDI-TOF instrument using 2,4,6-trihydroxyacetophenone as the matrix.

Table 4. Crystallographic Data for **1**

chemical formula	$C_{18}H_{26}N_3O_4PRu$
fw	480.16
cryst syst	orthorhombic
space group	$P2_12_12_1$
a (Å)	11.2523(5)
b (Å)	11.2529(5)
c (Å)	15.8614(8)
α (deg)	90
β (deg)	90
γ (deg)	90
V (Å^3)	2008.39(16)
Z	4
D_{calcd} (g cm^{-3})	1.589
F(000)	984
μ (mm^{-1})	0.889
T (K)	140(2)
wavelength (Å)	0.710 73
measd reflns	12 413
unique reflns	3529
unique reflns [$I > 2\sigma(I)$]	3327
no. of data/restraints/param	3529/0/247
R1[a] [$I > 2\sigma(I)$]	0.0195
wR2[a] (all data)	0.0427
GOF[b]	0.997

[a] $R1 = \sum||F_o| - |F_c||/\sum|F_o|$, $wR2 = \{\sum[w(F_o^2 - F_c^2)2]/\sum[w(F_o^2)^2]\}^{1/2}$. [b] $GOF = \{\sum[w(F_o^2 - F_c^2)2]/(n - p)\}^{1/2}$ where *n* is the number of data and *p* is the number of parameters refined.

(c) Determination of pK_a Values. The titration curves were fitted to the Henderson−Hasselbalch equation with the assumption that the observed chemical shifts are weighted averages according to the populations of the protonated and deprotonated species. The resonance frequencies change smoothly with pH between the chemical shifts of the charged form HA^+, stable in an acidic solution, and those of the neutral, deprotonated form A, which is present at high pH. At any pH, the observed chemical shift is a weighted average of the two extreme values $\delta(HA^+)$ and δ(A). The midpoint of the titration occurs when the concentrations of the acid and its conjugate base are equal: $[HA^+] = [A]$, i.e., when the pH equals the pK_a of the compound.

$$\delta_{av} = \frac{\delta(HA^+)[HA^+] + \delta(A)[A]}{[HA^+] + [A]}$$

The p*D* values of the NMR samples in D_2O were measured at 298 K, directly in the NMR tube, using a 713 pH meter (Metrohm) equipped with an electrode calibrated with buffer solutions at pH 4, 7, and 9. The p*D* values were adjusted with dilute DCl and NaOD. The pH at the midpoint of the curve is corrected by subtracting 0.44 from the p*D* values because the measurements were made in D_2O.[26]

(d) Cell Culture. Human MCF-7 breast carcinoma, T47D breast carcinoma, A549 lung carcinoma, and HT-29 colon carcinoma cell lines were obtained from the American Type Culture Collection, Manassas, VA. All other cell culture reagents were obtained from Gibco-BRL, Basel, Switzerland. The cells were routinely grown in a DMEM medium containing 4.5 g/L glucose, 10% foetal calf serum (FCS), and antibiotics at 37 °C and 6% CO_2. For the MTT tests, the cells were seeded in 48-well plates (Costar, Integra Biosciences, Cambridge, MA) as monolayers for 24−48 h in a complete medium to reach confluence, then a fresh complete

(22) *CrysAlis RED;* Oxford Diffraction Ltd.: Abingdon, U.K.
(23) Altomare, A.; Burla, M. C.; Camalli, M.; Cascarano, G. L.; Giacovazzo, C.; Guagliardi, A.; Moliterni, A. G. G.; Polidori, G.; Spagna, R. *J. Appl. Crystallogr.* **1999**, *32*, 115−119.
(24) Walker, N.; Stuart, D. *Acta Crystallogr. A* **1983**, *39*, 158−166.
(25) *Diamond*,version 3.0a; Crystal Impact GbR: Bonn, Germany.
(26) Mikkelsen, K.; Nielsen, S. O. *J. Phys. Chem.* **1960**, *64*, 632−637.

medium with 5% FCS was added together with the drugs, and the culture was continued for another 72 h. The test (see below) was performed for the last 2 h without changing the culture medium.

(e) Determination of Cell Viability. The compounds were dissolved directly in a culture medium to the required concentration. Cell viability was determined using the MTT assay, which allows the quantification of the mitochondrial activity in metabolically active cells.[27] Following drug exposure, MTT (final concentration 0.2 mg/mL) was added to the cells for 2 h, then the culture medium was aspirated, and the violet formazan precipitate was dissolved in 0.1 N HCl in 2-propanol. The optical density, which is directly proportional to the number of surviving cells, was quantified at 540 nm using a multiwell plate reader (iEMS Reader MF; Labsystems, Waltham, MA), and the fraction of surviving cells was calculated from the absorbance of untreated control cells.

Acknowledgment. We thank the Roche Research Foundation, the Swiss Cancer League, the Swiss National Science Foundation, and the EPFL for financial support. We also thank Dr. Evelyne Müller (EPFL) for assistance with the MALDI-TOF MS experiments.

Supporting Information Available: X-ray crystallographic data in CIF format. This material is available free of charge via the Internet at http://pubs.acs.org.

IC061008Y

(27) Mosmann, T. *J. Immunol. Methods* **1983**, *65*, 55−63.